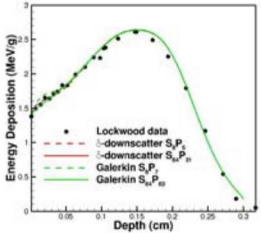
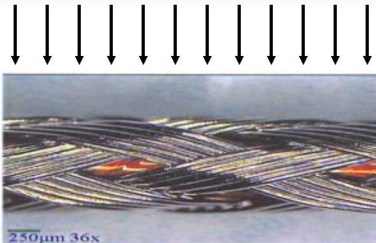


Exceptional service in the national interest

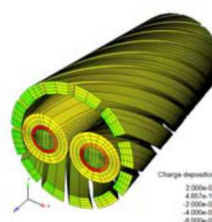
 Sandia
National
Laboratories



Graph showing Energy Deposition (MeV/g) versus Depth (cm). The data points (black dots) show a peak around 0.15 cm. Three theoretical curves are plotted: Lockwood data (dashed red), downscatter $S_{\mu\mu}P_{\mu\mu}$ (dashed green), and Galerkin $S_{\mu\mu}P_{\mu\mu}$ (solid green). The peak energy deposition is approximately 2.5 MeV/g at a depth of about 0.15 cm.



Micrograph showing a cross-section of a sample with a scale bar of 250 μm 36x. Below the image is the text "250 μm 36x".



3D visualization of charge deposition in a cylindrical sample. The color scale indicates charge deposition values, ranging from 0.000e+00 (blue) to 2.000e-03 (red). A legend on the right shows the color mapping for these values.

Specializations in the SCEPTRE Code for Charged-Particle Transport

Clif Drumm, Wesley Fan and Shawn Pautz
Radiation Effects Theory Dept. Sandia National Laboratories
RPSD 2018 Santa Fe, NM
27 August, 2018

Sandia National Laboratories is a multimission laboratory managed and operated by National Technology and Engineering Solutions of Sandia, LLC., a wholly owned subsidiary of Honeywell International, Inc., for the U.S. Department of Energy's National Nuclear Security Administration under contract DE-NA0003525.

 Sandia
National
Laboratories

Overview

- Methods for handling highly-forward-peaked scattering
- Methods for handling slow convergence of scattering source iterations
- Development activities
 - Discontinuous finite elements (DFE) in energy applied to the Continuous-Slowing-Down (CSD) term
 - Transport in the presence of ElectroMagnetic (EM) fields

2

Methods for Handling Highly-Forward-Peaked Scattering



- Legendre polynomial expansion alone inadequate
- Explicit δ -function down-scatter term (extended transport correction)
- Galerkin mapping between angular flux and angular moments

3

Explicit δ -Function Downscatter



$$\sigma_{g' \rightarrow g}(\mu_0) \cong \sum_{l=0}^L \tilde{\sigma}_{g' \rightarrow g}^l, P_l(\mu_0) + \sigma_{g' \rightarrow g}^{L+1} \delta(1 - \mu_0)$$

- Down-scatter source depends upon the angular moments *and* angular flux

$$\Omega \cdot \nabla \psi_g + \sigma_{t,g} \psi_g = \sum_{l,g'} \left\{ [M] \left[\tilde{\Sigma}_{g' \rightarrow g}^l \right] \phi_{g'} + \left[\Sigma_{g' \rightarrow g}^{L+1} \right] \psi_{g'} \right\} + Q_g$$

$[M]$ is the moment-to-discrete operator

$\left[\tilde{\Sigma}_{g' \rightarrow g}^l \right]$ and $\left[\Sigma_{g' \rightarrow g}^{L+1} \right]$ are the diagonal scattering cross section matrices

4

Galerkin Mapping Between Angular Flux and Angular Moments



- Discrete-to-moment operator $[D]$ is the inverse of the moment-to-discrete operator $[M]$
- Similarity transformation of the (diagonal) scattering moments matrix
- Requires that the number of scattering moments be equal to the number of angular quadrature directions

$$\Omega \cdot \nabla \psi_g + \sigma_{t,g} \psi_g = \sum_{l,g'} [M] \left[\Sigma_{g' \rightarrow g}^l \right] [M]^{-1} \psi_{g'} + Q_g$$

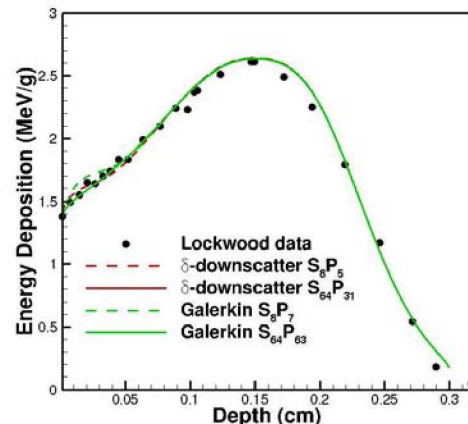
J. MOREL, "A Hybrid Collocation-Galerkin-Sn Method for Solving the Boltzmann Transport Equation," *Nucl. Sci. Eng.*, **101**, 72 (1989).

5

Energy Deposition Compared with Lockwood Data



- 1-MeV electrons on range-thick Be
- Good agreement except for low-order Galerkin



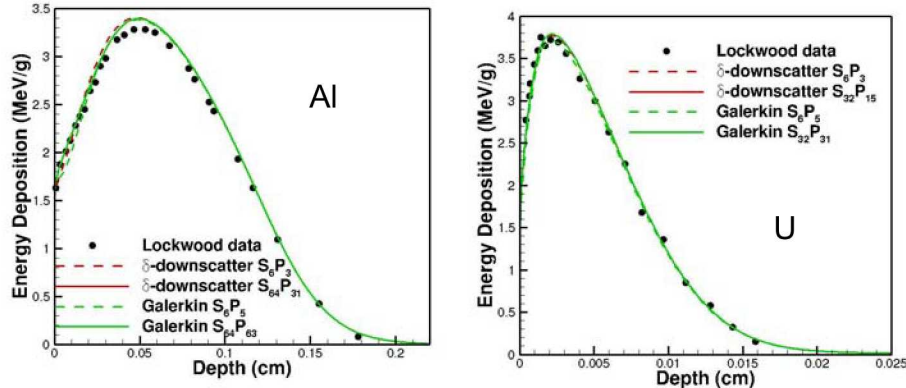
G. LOCKWOOD, L. RUGGLES, G. MILLER and J. HALBLEIB, "Calorimetric Measurement of Electron Energy Deposition in Extended Media- Theory vs Experiment," Sandia National Laboratories report, SAND79-0414, Albuquerque, NM (reprinted 1987).

6

Energy Deposition Compared with Lockwood Data



- 1-MeV electrons on range-thick Al and U



Methods for Handling Slow Convergence of Scattering-Source Iterations



- Charged-particle cross sections have large scattering ratios resulting in slow convergence of source iterations
- SCEPTRE includes multiple solver options that perform well for problems including cross sections with large scattering ratios
- Alternative solvers perform well as accelerators (Transport Synthetic Acceleration, TSA)

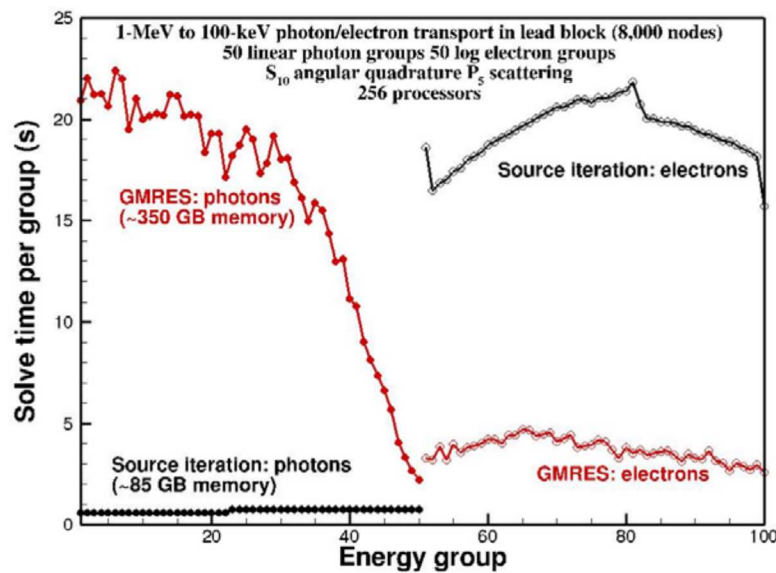
SCEPTRE Contains Multiple Solver Options



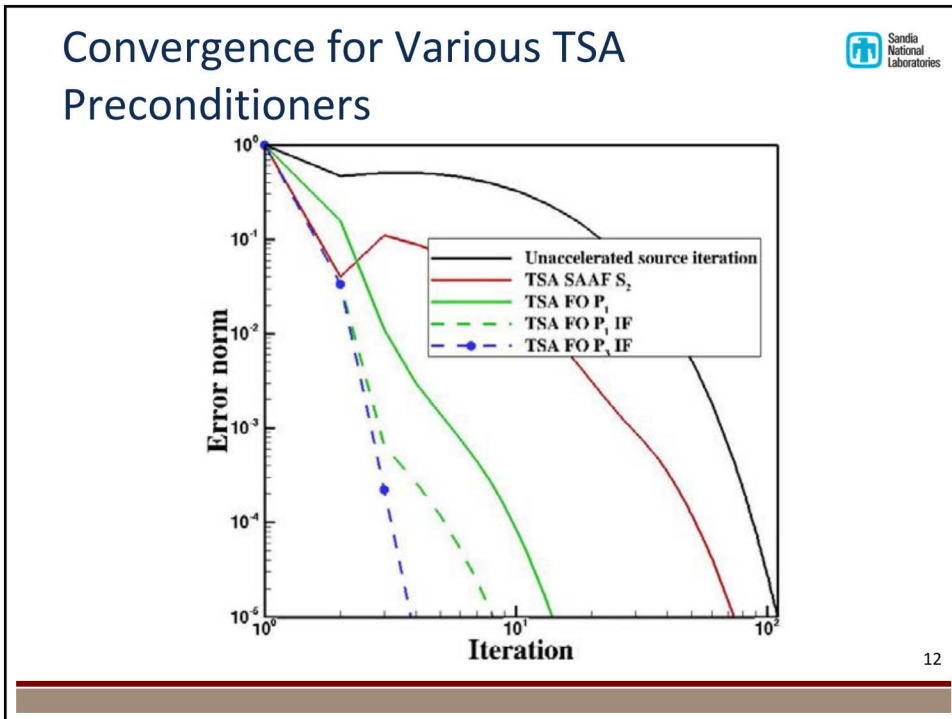
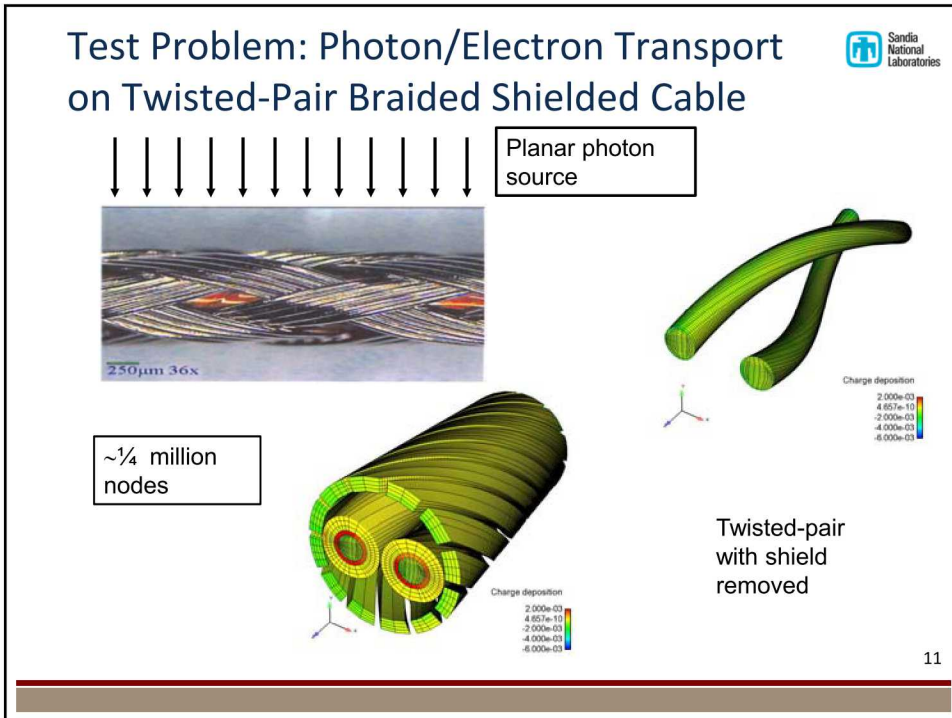
- Traditional sweeps-based solver using source iteration
 - Fast for photons
 - Slow for electrons
 - Small memory requirement
- Simultaneous space-angle Krylov solvers
 - Fast for electrons
 - Slow for photons
 - Large memory requirement
 - Multiple solver options
 - S_N or P_N angular treatment
 - Self-Adjoint Angular Flux (SAAF) or Least-Squares (LS) utilizing continuous spatial finite elements
 - 1st-order transport utilizing discontinuous spatial finite elements

9

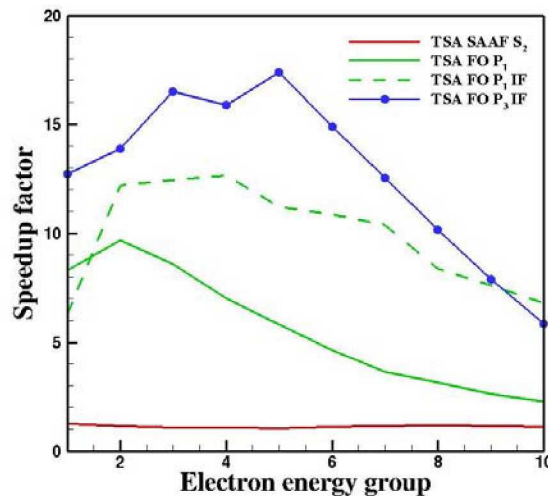
Comparison of Timing Results



10



Speed-Up Factors for Various TSA Preconditioners



13

Speed Up Depends on Details of the Coarse-Level Solves



TSA method	Coarse-level parameters				Total solve time of electron groups (s)	Speed up
	Preconditioner	Convergence tolerance	Max iterations			
none	-	-	-		3530	1
FO P ₁	none	0.01	100		653	5.4
FO P ₁	IF	0.01	10		365	9.7
FO P ₃	IF	0.01	10		272	13.
SAAF S ₂	none	10 ⁻⁴	1000		3160	1.1

14

Finite-Elements in Energy

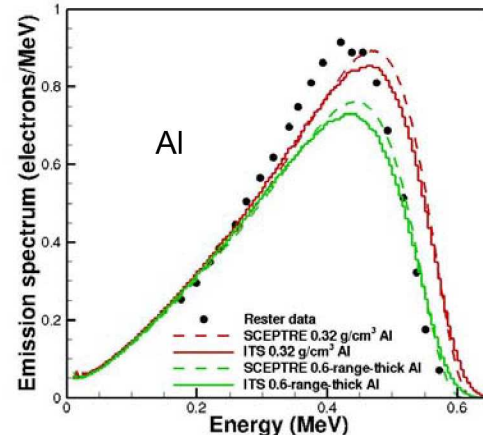


- Effective for modeling the Continuous-Slowing-Down (CSD) term
- Requires FE weighted cross sections and stopping powers
- SCEPTXS code is being developed to replace CEPXS to include FE weighted data

15

Electron Emission Spectrum (Rester Data)

- Electron emission spectrum sensitive to the aluminum thickness



D. RESTER and J. DERRICKSON, "Electron Transmission Measurements for Al, Sn, and Au Targets at Electron Bombarding Energies of 1.0 and 2.5 MeV," *J. App. Phys.*, **42**, 714 (1971).

16

Charged-Particle Transport in the Presence of EM Fields



- Relativistic Vlasov equation

$$\begin{aligned}
 & \frac{1}{v} \frac{\partial \psi}{\partial t} + \boldsymbol{\Omega} \cdot \nabla \psi + \sigma \psi + q(\boldsymbol{\mathcal{E}} \cdot \boldsymbol{\Omega}) \left[\frac{\partial \psi}{\partial E} - \frac{1 + 4\beta^2}{\mathcal{D}(E)} \psi \right] \\
 & + \frac{q}{\mathcal{D}(E)} [\mathcal{E}_x(1 - \mu^2) - \mathcal{E}_y \mu \eta - \mathcal{E}_z \mu \xi + v(B_z \eta - B_y \xi)] \frac{\partial \psi}{\partial \mu} \\
 & + \frac{q}{\mathcal{D}(E)(1 - \mu^2)} [\mathcal{E}_z \eta - \mathcal{E}_y \xi + v(B_y \mu \eta + B_z \mu \xi - B_x(1 - \mu^2))] \frac{\partial \psi}{\partial \varphi} = Q
 \end{aligned}$$

$$\mathcal{D}(E) = \frac{E(E + 2m_0c^2)}{E + 2m_0c^2}$$

$$\begin{aligned}
 \boldsymbol{\mathcal{E}} &= \mathcal{E}_x \mathbf{i} + \mathcal{E}_y \mathbf{j} + \mathcal{E}_z \mathbf{k} \\
 \boldsymbol{B} &= B_x \mathbf{i} + B_y \mathbf{j} + B_z \mathbf{k}
 \end{aligned}$$

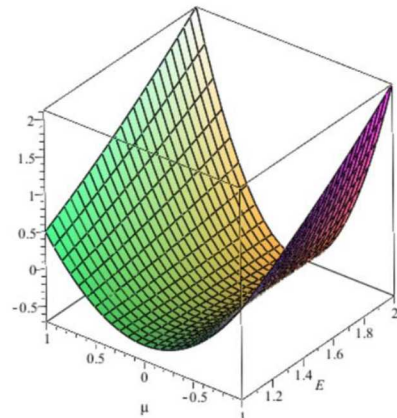
17

Simple Method of Manufactured Solutions (MMS) Test Problem



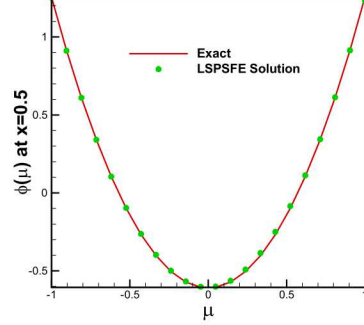
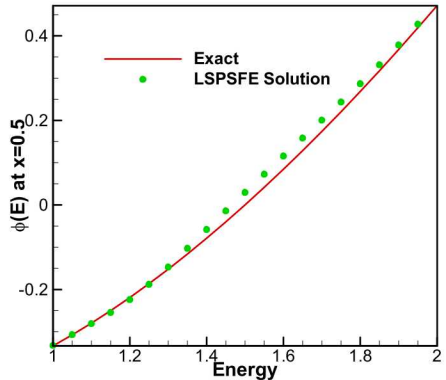
- 1D
- Void
- Uniform electric field
- No magnetic field

$$\psi(x, \mu, E) = \sqrt{E}(\mu^2 E - x)$$



18

Least-Squares Phase-Space FE (LSPSFE) Solution



19

Conclusions



- Productization of new capabilities
 - Finite-elements in energy
 - Finite elements in angle
 - Transport in the presence of EM fields
- More experience with acceleration/preconditioning methods
 - Some problems resist acceleration
 - Many knobs to turn to get effective speedup
- New weighted cross section/stopping power
 - Energy weighted for energy finite elements
 - Angular weighted for angular finite elements

20